2008 American Control Conference
Westin Seattle Hotel, Seattle, Washington, USA
June 11-13, 2008

CONTROL OF A REVERSE OSMOSIS DESALINATION PROCESS AT HIGH RECOVERY

Charles W. McFall, Alex Bartman, Panagiotis D. Christofides, and Yoram Cohen

Abstract— **Feed-forward/feedback control techniques that utilize Lyapunov-based control laws are implemented on a high recovery reverse osmosis desalination plant model. A detailed mathematical model of a high recovery reverse osmosis plant is developed. This model incorporates the large spatial variations of concentration and flow-rate that occur in membrane units during high recovery operation. Bounded nonlinear feedback and feed-forward controllers are developed and applied to this system. The application of these controllers is demonstrated in the context of a high recovery reverse osmosis process simulation. The scenarios demonstrate the ability to compensate for the effects of large time varying disturbances in the feed concentration on specific process outputs with feed-forward/feedback control.**

I. INTRODUCTION

System automation and reliability are crucial components of any modern reverse osmosis (RO) plant. The operational priorities are personnel safety and product water quality, while also meeting environmental and economic demands. It is highly desirable to operate RO processes at high recovery, where most of the feed water volume is processed to low salinity product water, due to decreased environmental and economic costs associated with brine disposal [1], [2]. Automated RO plants that operate at high recovery, however, can become more vulnerable to disturbances in feed water quality, total dissolved solids (TDS) concentrations, and temperature. Such disturbances often appear in usual feed water sources, due to temporal and spatial variations [3], [4]. These disturbances can cause undesirable behavior in product flow-rate, internal system pressure, and brine flow-rate.

Several contributions have been made in the literature to process control of RO systems. The first paper which proposed an effective closed-loop control strategy for RO utilized multiple SISO control-loops [5]. Step tests were used to perform system identification, resulting in a model that is a linear approximation around the operating point. The control algorithm of MPC was applied to the resulting linear model in [6] and [7]. Experimental system identification and MPC applications can also be found in [8] and [9]. The work of [10] and [11] implements minimal feedback control on RO desalination systems, powered by renewable energy sources, in the form of digital on/off switching. Some hybrid systems modeling and control work has been published, such as in [12]. A steady-state model similar to the one developed in this work can be found in [13]. Preliminary results on fault tolerant control of RO systems can be found in [14]. Despite these efforts, at this stage there has been no work on model based control for high recovery RO processes.

The goal of this work is to develop model based nonlinear feed-forward/feedback control structures for high recovery RO while accounting for such practical issues as sampled measurements and large time-varying feed disturbances. In order to accomplish this goal a detailed mathematical model of a high-recovery RO plant must first be developed. This model must adequately describe the evolution of process states in time, and it must also account for the spatial variation of TDS and flow-rate inside the membrane units. Most RO models simple enough for control purposes, such as those found in [15], consider a well mixed model with a single value for concentration on the retentate side of the membrane. However, under high recovery operation the gradients along the length of the membrane unit can be quite significant. As fluid flows axially along the module the bulk concentration increases, the flow rate decreases, and the local permeate flux decreases [13]. The model developed in the present work includes appropriate differential equations that account for these gradients. A Lyapunov-based nonlinear controller is then applied to this high recovery RO model. One of the main objectives of a controller in high recovery RO is to reject disturbances caused by feed water variation. Feed disturbances could cause undesired fluctuations in the product flow rate or the internal pressure. To accomplish disturbance rejection, the control law includes both feedback and feed-forward components. The feed water stream concentration can easily be measured in practice, so the examples presented in this work explore the ability of the proposed control method to reject such disturbances.

II. PROCESS DESCRIPTION AND MODELING

Fig.1 shows a schematic of an elementary RO desalination process. This is a single-unit RO system with no pre-treatment or post-treatment units. Feed brackish or seawater enter the system through the high pressure pump. This high pressure water then flows across an RO membrane, and low salinity product water permeates through the membrane. Concentrated brine then exits the membrane module and passes through a throttling valve to be discharged at atmospheric pressure. The RO plant consists of a high pressure pump, two automated valves, a spiral wound membrane unit, required plumbing, and tanks. The valve settings can be manipulated in real time based on measurement information which includes the flow velocities and feed concentration.

The first principles model of this system is based on a macroscopic kinetic energy balance, a local mass balance,

Department of Chemical and Biomolecular Engineering University of California, Los Angeles, CA 90095
Corresponding author is P. D. Christofides pdc@seas.ucla.edu

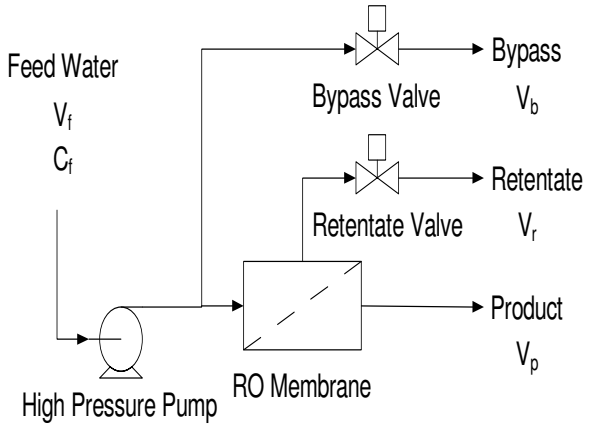

Fig. 1. Single membrane unit high recovery reverse osmosis desalination process. The two actuated valves act as manipulated inputs.

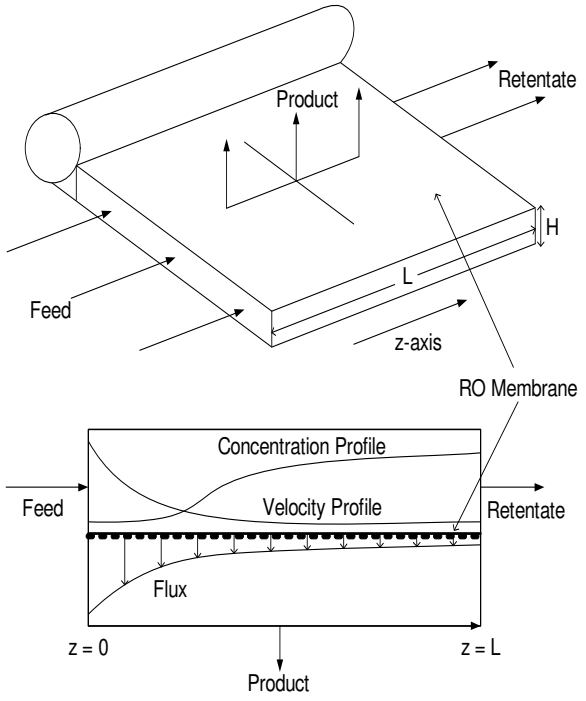

Fig. 2. An expanded view of a spiral wound membrane module and typical concentration and velocity profiles inside the module.

and a microscopic mass shell balance. This model assumes an incompressible fluid and constant internal volume and mass. It is assumed that the water in the module travels in a plug flow with no back-mixing or axial diffusion. It is also assumed that the retentate TDS in the membrane module can be approximated by a linear relation to the osmotic pressure [16]. Skin friction through the piping and the membrane module are considered negligible relative to the hydraulic losses in the throttling valves and across the membrane.

The energy balance consists of two nonlinear ordinary differential equations (ODEs) in time where the velocities of the bypass and retentate stream are the states. Each ODE is derived from an energy balance around an actuated control valve [17]. Two ODEs that can describe the process depicted in Fig. 1 take the form:

$$\begin{aligned} \frac{dv_b}{dt} &= \frac{A_p}{\rho V}(P - \tfrac{1}{2}v_b^2 e_{v1}) \\ \frac{dv_r}{dt} &= \frac{A_p}{\rho V}(P - \tfrac{1}{2}v_r^2 e_{v2}) \end{aligned} \tag{1}$$

where v_b is the bypass velocity, v_r is the retentate velocity, A_p is the pipe cross sectional area, V is the total internal volume, ρ is the fluid density, and P is the internal pressure. e_{v1} and e_{v2} are friction loss factors for the actuated valves and act as manipulated inputs. These two ODEs are not explicitly coupled, however, coupling does occur through the pressure term, P. In this work the skin friction is assumed negligible, and this assumption is reasonable for systems with high internal pressure, and a short pipe runs such that the pressure drop due to skin friction is small compared to the internal pressures. In this case, P takes the same value from the pump to the valves. The external pressure is taken as atmospheric pressure. P in this work is an algebraic variable whose value depends on the system states and changes with time. P is a function of feed concentration C_f, v_b, and v_r. Specifically, P at each time is obtained via solving a local mass balance and a microscopic mass shell balance in space. The local mass balance around the bypass line and feed line junction allows the calculation of the feed velocity to the membrane module, v_{mf}, given the bypass and retentate velocities from (1):

$$v_f = v_b + v_{mf} \tag{2}$$

where v_f is the constant velocity of the feed stream.

It is critical in a high recovery system, where the concentration and velocity in the module change significantly along the axis of flow, to accurately describe the concentration and velocity profiles along the membrane module. In order to model these profiles a shell balance is performed across the membrane to generate a two state ODE system. An expanded view of an unwound spiral-wound membrane module and a drawing depicting typical concentration and velocity profiles in a module can be seen in Fig. 2. The internal compartment of the membrane module is simplified to a rectangular space. A steady-state shell balance is performed on this space assuming radially well mixed plug flow. A quasi-steady state assumption is made on this system such that disturbances on the system will have a time scale that is slow relative to the time scale of the plug flow in the membrane unit. It is possible to extend these results to include a transient term in the shell balance, where P still remains an algebraic variable. The shell balances are based on the conservation of TDS mass and water mass inside the membrane module. The differential volume for the shell balance has the dimensions W by H by δz, where δz is an infinitesimal length in the z direction. W is the membrane width ($W = A_m/L$, A_m is the membrane area). The derivation assumes that dissolved solids are completely rejected, and that only water

permeates the membrane at a flux approximated by $J_w = K_m(P - K_{\Delta\pi}C_z)$, where J_w is the permeate flux, K_m is the overall mass transfer coefficient, $K_{\Delta\pi}$ is a constant that relates TDS to osmotic pressure, and C_z is the concentration along the z-axis in the membrane. The result of the shell balance is the following two coupled ODEs in space and three boundary conditions (owing to the fact that P is an algebraic variable):

$$\begin{aligned} \frac{dC_z}{dz} &= \frac{C_z}{v_z}\frac{K_m(P - K_{\Delta\pi}C_z)}{\rho H} \\ \frac{dv_z}{dz} &= -\frac{K_m(P - K_{\Delta\pi}C_z)}{\rho H} \\ C_z(z{=}0) &= C_f \\ v_z(z{=}0) &= \alpha v_{mf} \\ v_z(z{=}L) &= \alpha v_r \end{aligned} \tag{3}$$

where z is the direction of flow through the membrane, v_z is the velocity of flow in the membrane along the z-axis, and H is the height of the membrane channel. The boundary conditions arise when (3) is coupled with (1) and (2). Equation (3) is solved at each time step as we integrate (1) in time. The solution to the ODEs of (3) is complicated by the fact they must satisfy three boundary conditions, two at the inlet, and one at the outlet owing to the fact that P is an unknown algebraic variable. The feed concentration, C_f, represents a boundary condition at $z = 0$ (at the membrane inlet) provided as a time varying parameter. The feed velocity to the module, v_{mf}, provides the velocity boundary condition at $z = 0$. Retentate velocity, v_r, provided from (1) is a boundary condition at the membrane outlet, $x = L$, where L is the membrane length in the z direction. The parameter α is the ratio of the pipe cross sectional area to the membrane channel cross sectional area. Pressure is the unknown variable in time that must be altered in order to find the solution to (3). The solution to (3) is found at each time by using a type of shooting method [18] where the system pressure is adjusted until all three boundary conditions are satisfied. This system pressure is then plugged into (1) for the next step forward in time.

A step-by-step discussion of the algorithm used to compute the solution of the open-loop model of (1), (2), and (3) is presented to clarify the method employed in this work. An assumption is made that the profiles of C_z and v_z change only with respect to z within each integration step in time. It is also assumed that C_f changes slowly relative to the residence time in the module. This allows the independent solution of (3) at each time. In order to satisfy this requirement practically, measurements must be taken on a faster time scale than rate of change of the feed disturbance. Also, residence time in the module must be short compared to the feed disturbance time scale. A large well-mixed holding tank placed before the feed can act as a filter to eliminate fast time-scale disturbances.

In order to solve the system of equations presented in (1), (2), and (3) numerically, the following algorithm is applied.

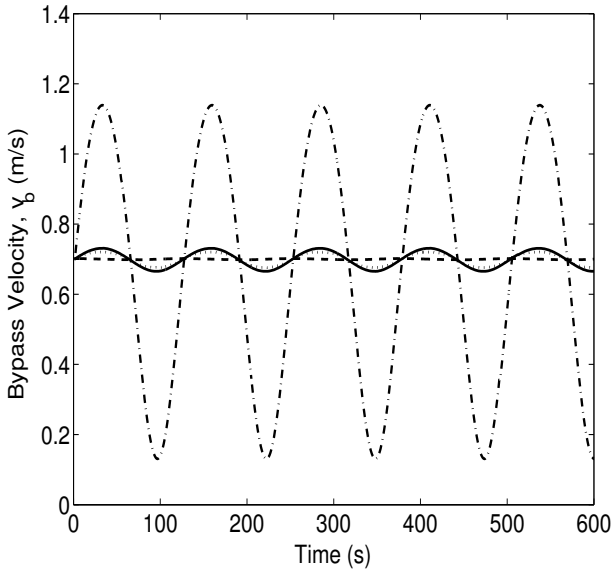

Fig. 3. Bypass velocity, v_b, profiles versus time; Open-loop (solid line), closed-loop feedback control (dotted), feed-forward/feedback control with v_b and v_r as controlled outputs (dashed), feed-forward/feedback control with P and v_r as controlled outputs (dash-dotted).

1) Initial conditions for v_b and v_r are chosen.
2) v_{mf} is computed from (2).
3) Given v_{mf}, C_f, and a guess value for P, a solution to (3) is computed numerically.
4) The resulting $v_z(z{=}L)$ is compared to αv_r, and P is adjusted via shooting method until $v_z(z{=}L)$ is equal to αv_r.
5) The value of P resulting from step 4 is used in (1) to integrate numerically one step forward in time.
6) The results of step 5 provide updated values of the states, v_b and v_r, and the algorithm returns to step 1 using these values as new initial conditions. This process is repeated until the desired integration time is reached.

The open-loop simulation results can be seen as the solid line in Figs. 3 through 6. The simulation is run at high recovery for a time of 10 min with a time varying disturbance on C_f as defined in Table I. While this disturbance is at a higher frequency than would usually occur in practice, the ability to reject this disturbance will in general signify a control method that is also able to handle lower frequency disturbances. It can been seen that v_b and v_p oscillate due to the disturbance, but the oscillations are not large relative to the steady-state values for these states. However, Fig. 5 shows wide swings in the internal pressure for the open-loop case. This type of behavior could lead to safety issues if the pressure exceeds the safety rating of hoses, fittings, or pressure vessels. This motivates the use of feedback control to reduce the effects of feed disturbances on the process.

The potential manipulated inputs to the system are the friction loss factors for the valves (e_{v1} and e_{v2}). Valves can be manipulated in practice by an automated electric motor that partially opens or closes the valves. The measured

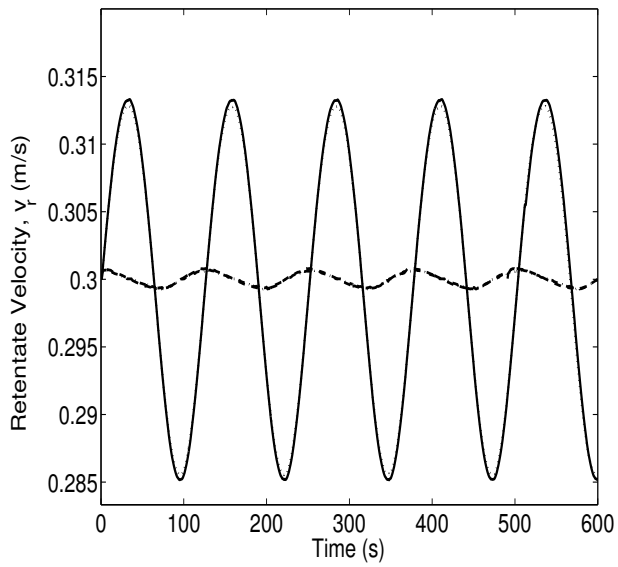

Fig. 4. Retentate velocity, v_r, profiles versus time; Open-loop (solid line), closed-loop feedback control (dotted), feed-forward/feedback control with v_b and v_r as controlled outputs (dashed), feed-forward/feedback control with P and v_r as controlled outputs (dash-dotted). The dash-dotted and dashed line overlap in this figure.

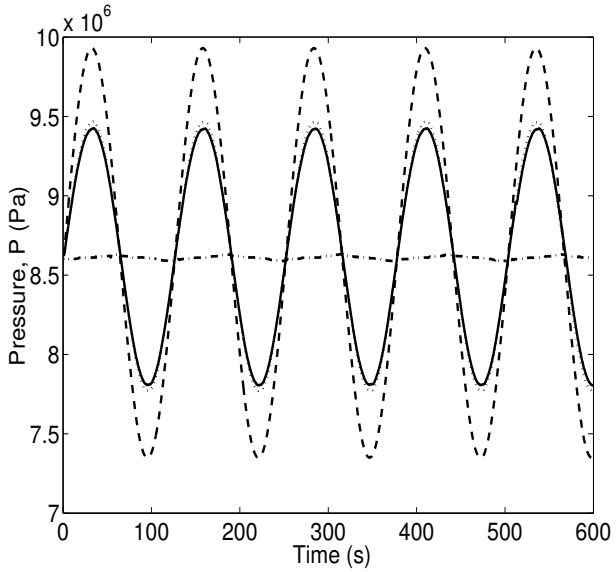

Fig. 5. Internal pressure, P, profiles versus time; Open-loop (solid line), closed-loop feedback control (dotted), feed-forward/feedback control with v_b and v_r as controlled outputs (dashed), feed-forward/feedback control with P and v_r as controlled outputs (dash-dotted).

outputs are the bypass velocity (v_b), retentate velocity (v_r), and internal pressure (P). The super script ss corresponds to the high recovery steady-state values for this system when $C_f^{ss} = 10000\ mg/L$, a brackish feed water source. Operation at this point provides a recovery of 91%.

TABLE I
PROCESS PARAMETERS AND STEADY–STATE VALUES

ρ	=	1000	kg/m^3
V	=	0.01	m^3
v_f	=	4.0	m/s
A_p	=	1.27	cm^2
A_m	=	13	m^2
K_m	=	9.218×10^{-9}	s/m
$K_{\Delta\pi}$	=	78.7	$Pa/(mg/L)$
C_f	=	$10000 + 1500\sin(0.05t)$	mg/L
H	=	1.0	mm
L	=	5.0	m
α	=	0.049	
C_f^{ss}	=	10000	mg/L
e_{v1}^{ss}	=	3.57×10^7	
e_{v2}^{ss}	=	1.92×10^8	
v_b^{ss}	=	0.7	m/s
v_r^{ss}	=	0.3	m/s
v_p^{ss}	=	3.0	m/s
P^{ss}	=	8.61×10^6	Pa

One control objective is to stabilize the process at the desired retentate velocity, v_r, and operating pressure, P, in the presence of large time varying disturbances in the feed concentration C_f. This configuration would be used on a system that operates close to the maximum allowable internal pressure. The internal pressure often needs to be below a specified value for safety reasons (safety ratings for fittings and pressure vessels), and at high recovery an RO plant may operate close to this safety threshold. Another control objective could be to stabilize the process at the desired retentate velocity, v_r, and desired product flow rate, v_p. This type of disturbance rejection may be used on RO systems that are designed for extremely high pressures, and allows for a consistent delivery of product water. The controller will use both e_{v1} and e_{v2} as manipulated inputs.

III. FEEDBACK CONTROLLER SYNTHESIS

To present results in a convenient form, the model of (1) is written in a deviation variable form around the desired steady state. This is defined as $x = [x_1\ x_2]^T$ where $x_1 = v_b - v_b^{ss}$ and $x_2 = v_r - v_r^{ss}$. The plant can then be described by the following non linear continuous-time system:

$$\begin{aligned} \dot{x}(t) &= f(x(t)) + g(x(t))u(t) + w(x(t))d(t) \\ |u_i| &\leq u_i^{max} \end{aligned} \tag{4}$$

where $x(t) \in \Re^2$ denotes the vector of process state variables, $u(t)$ is a vector of inputs where $u(t) \in [-u_i^{max}, u^{max}] \subset \Re^2$ denotes the i^{th} constrained manipulated input, $u_1(t) = e_{v1} - e_{v1}^{ss}$ and $u_2(t) = e_{v2} - e_{v2}^{ss}$, and $d(t)$ denotes the disturbance on the system, $d(t) = P - P^{ss}$. The disturbance in this system originates from the feed concentration, C_f, but $d(t)$ is expressed in terms of P because C_f acts on P through (3). The value of u_i^{max} is taken as 5×10^9. The numerical values of u can become quite large because the manipulated input represents a resistance to flow. A valve would be considered completely closed at an infinitely large value, and the value must be greater than zero which represents a completely open valve. The control objective is to maintain specific outputs at

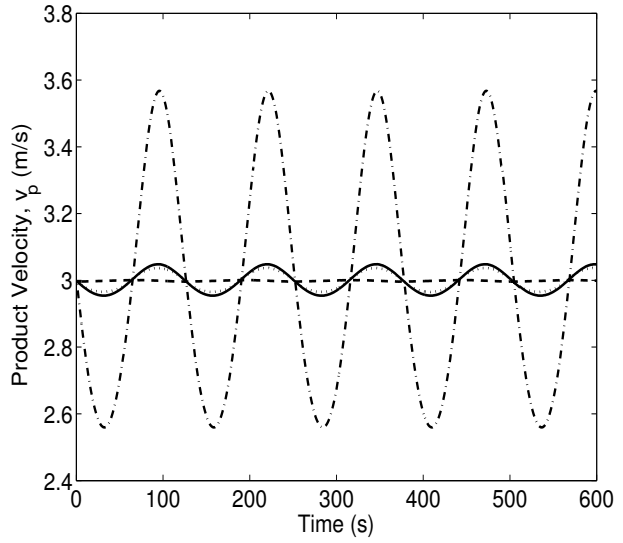

Fig. 6. Product velocity, v_p, profiles versus time; Open-loop (solid line), closed-loop feedback control (dotted), feed-forward/feedback control with v_b and v_r as controlled outputs (dashed), feed-forward/feedback control with P and v_r as controlled outputs (dash-dotted).

their desired values in the presence of large time varying disturbances on the feed concentration. The state feedback control problem where measurements of all process states are available for all times is considered because these velocities can be readily measured in practice. $d(t)$ is available as a measurement of C_f, and C_f can be used to calculate P, and hence, $d(t)$. Since $d(t)$ is readily available $\hat{f}(x(t)) = f(x(t)) + w(x(t))(d(t))$ is defined.

Next, a Lyapunov-based controller that enforces asymptotic stability in the presence of actuator constraints is synthesized. First a quadratic Lyapunov function of the form $V_L = x^T P_L x$ is defined where P_L is a positive-definite symmetric matrix. This Lyapunov function is used to synthesize a bounded nonlinear feedback control law (see [19], [20], and [21]) of the form:

$$u_k = -r(x, u^{max}) L_g V_L \tag{5}$$

where

$$r = \frac{L_{\hat{f}}^* V_L + \sqrt{(L_{\hat{f}}^* V_L)^2 + (u^{max}|L_g V_L|)^4}}{(|L_g V_L|)^2 (1 + \sqrt{1 + (u^{max}|L_g V_L|)^2})} \tag{6}$$

and $L_{\hat{f}}^* V_L = L_{\hat{f}} V_L + \alpha V_L$, $\alpha > 0$. L_f and L_g are the standard Lie derivatives for the vector functions f and g. The scalar function $r(\cdot)$ in (5) and (6) can be considered as a nonlinear controller gain.

If the value of $d(t)$ is available at each time this Lyapunov-based feedback controller includes a feed-forward compensation component. In this case the controller is updated with the latest disturbance information to reject the effects of the disturbance on the states, v_b and v_r. However, if the value of $d(t)$ is not available for measurement at each time, $P = P^{ss}$ for the control law and the controller acts in a standard Lyapunov-based feedback manner. In this case control action is not taken until the states have moved away from the steady-state values due to the disturbance, and the control action does not completely compensate for the disturbance.

IV. SIMULATION RESULTS

A. Feedback Control

The first simulation scenario involves using the Lyapunov-based control law presented in (5). This scenario considers the same disturbance as in the open-loop case. The states are sampled at a rate of one measurement per second. The control action for the manipulated inputs is computed once per second based on these measurements. This control action is implemented for the duration of the sample time, which is one second, in a sample-and-hold fashion. The disturbance is not measured in this case. The value of P used in $\hat{f}(x(t))$ is P^{ss} for all t, and the controller does not completely compensate for the disturbance on C_f.

The closed-loop simulation results can be seen as the dotted lines in Figs. 3 through 6. The manipulated inputs can be seen in Fig. 7. The states, v_b and v_r, and the product flow, v_p, oscillate at a marginally lower magnitude than those of the open-loop case, so the feed back control is able to slightly damp out the effects of the disturbance. If the gain on the controller is increased by changing P_L, it is possible to decrease the disturbance effect further at the expense of higher control actions and possible instability at this sampling rate. However, under closed-loop operation the pressure oscillates at a somewhat higher magnitude than the open-loop case, and this may not be acceptable for safety reasons. This type of feedback control may be useful for the case where regulating the states and product flow rate is more important than the internal pressure, for example, when the system is being operated at a pressure far below its rated maximum. However, the poor performance of feedback alone motivates the addition of feed-forward compensation to the controller that takes advantage of C_f measurements.

B. Feed-Forward/Feedback Control: v_b and v_r as Controlled Outputs

The second simulation scenario involves using the Lyapunov-based control law presented in (5), with feed-forward compensation. The advantage of controlling the states, v_b and v_r, at their steady state values is that the product flow rate, v_p also remains at the desired steady-state value due to conservation laws. For this scenario the time varying nature of C_f is the same as in the open-loop case. Measurements of the states and the disturbance, C_f, are sampled at a rate of one per second. At each sample time a control action is computed and implemented in a sample-and-hold fashion. At each sampling time (1), (2), and (3) are solved for the parameters contained in $\hat{f}(x(t))$ corresponding to the current C_f value and the desired v_p and v_r values. This can be done with the follow steps:

1) Choose set points for v_b and v_r, in this case 0.7 and 0.3 m/s respectively.

2) Solve (2) for v_{mf}.
3) Find the appropriate P, with shooting method, to satisfy all the boundary conditions for (3).
4) Set (1) equal to zero, and solve for e_{v1}^{nom} and e_{v2}^{nom}. These are the nominal values for the manipulated inputs that will compensate for the current disturbance, $C_f(t)$, and are components of $\hat{f}(x(t))$.

The control law in (5) is used to compute a feedback control action based on the current $\hat{f}(x(t))$ obtained from the above algorithm. This control action is added to the nominal e_{v1}^{nom} and e_{v2}^{nom} values, and implemented on the valves. This process is repeated at each sample time to obtain a feedback control action with feed-forward compensation. The manipulated inputs can be seen in Fig. 7 and compared to Fig. 7 the control actions are larger; yet they are within reasonable actuator limits.

The simulation results can be seen as the dashed lines in Figs. 3 through 6. The values of v_b, v_r, and v_p all stay very close to the steady-state points given in Table I, and the effects of the disturbance are effectively damped. A shorter sampling interval would reduce the disturbance effects even further. In this case, the value of P swings sharply in order to compensate for the changing feed conditions, $C_f(t)$. To achieve the desired recovery of over 90% even when the $C_f(t)$ is much higher than C_f^{ss} requires very high pressures. This application would be desirable only when product flow rate is a critical parameter that cannot be disturbed, and the RO system is designed to handle such high internal pressures.

C. Feed-Forward/Feedback Control: P and v_r as Controlled Outputs

The third simulation scenario does not fall directly under the Lyapunov-based feedback/feed-forward framework utilized in the previous two simulations, however, it is an important one from a practical point of view. For safety reasons, the large internal pressures exemplified in the previous examples motivate the use of feed-forward compensation that maintains $P(t)$ at a constant value, P^{ss}. In order to accomplish this, another variable (either v_b or v_r) must be used to compensate for the effects of C_f. v_r is often constrained due to the membrane module capacity, so v_b is an excellent candidate for this role. The bypass velocity can vary widely with little to no ill effect on the system: v_b is readily recycled, there are usually no downstream lines that depend on v_b, and there are no safety issues associated with wide v_b variations.

The third simulation scenario involves using a Lyapunov-based control law similar to the one presented in (5). Again, C_f is the same as the previous scenarios, and measurements of the states and disturbance are obtained at a rate of one sample per second. Given current data acquisition and control hardware this is a reasonable sampling rate, and in practice sampling could be much more frequent. The control action is implemented in a sample-and-hold fashion.

The framework for the feedback control with feed-forward compensation for P and v_r is slightly different than the one used in the previous two examples. At each sampling time

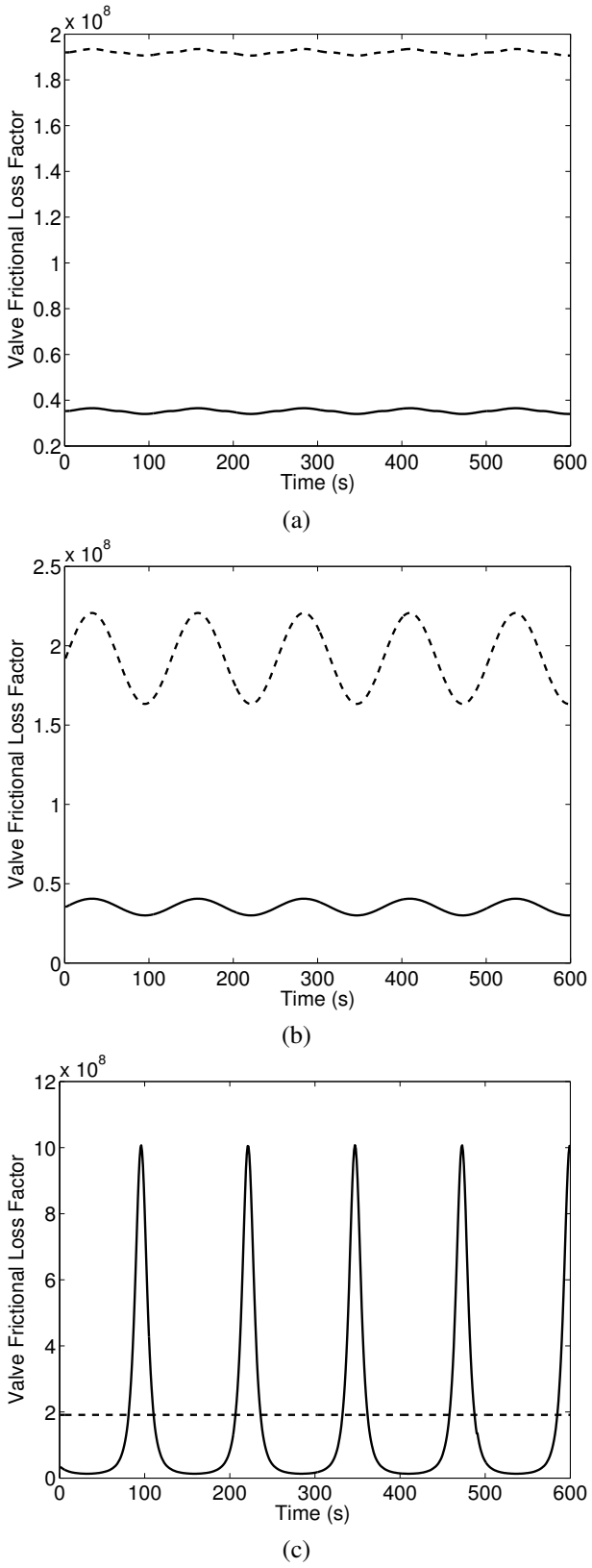

Fig. 7. Manipulated inputs for the Lyapunov-based feedback controller with no feed-forward compensation with v_b and v_r as the controlled outputs (a). Manipulated inputs for the feed-forward/feedback controller with v_b and v_r as the controlled outputs (b). Manipulated inputs for the feed-forward/feedback controller with P and v_r as the controlled outputs (c). e_{v1} is the solid line, and e_{v2} is the dashed line.

(1), (2) and (3) are solved for the steady-state corresponding to the current C_f value and the desired P and v_r values. This can be done with the following steps:

1) Choose set points for P and v_r, in this case $8.6 \times 10^6\ Pa$ and $0.3\ m/s$ respectively.
2) Solve (3) with the following two boundary conditions using shooting method where an initial guess is made on $v_z(z=0)$:
   a) $C_z(z=0) = C_f$
   b) $v_z(z=L) = \alpha v_r$
3) The resulting value of $v_z(z=0)$ from the previous step is used to calculate v_{mf}
4) v_{mf} is used with (2) to calculate a desired value for v_b. This v_b and the set point for v_r designate a new desired operating point where $P(t) = P^{ss}$
5) Set (1) equal to zero, substitute in the values for P, v_r, and v_b, and solve for e_{v1}^{nom} and e_{v2}^{nom}.

The control law in (5) is then used to compute a control action based on this new operating point provided from the above algorithm. This control action is added to the e_{v1}^{nom} and e_{v2}^{nom} values from the above algorithm, and implemented on the valves. This process is repeated at each sample time to obtain a new operating point and compute a control action that has feed-forward and feedback components. In other words, at each sampling time the steady state problem of (1), (2), and (3) is solved to find the desired operating point where $P(t) = P^{ss}$ and $v_r(t) = v_r^{ss}$, and a control action from a Lyapunov-based control law is implemented based on this new operating point. Manipulated inputs resulting from this framework, e_{v1} and e_{v2}, are shown in Fig. 7.

The closed-loop feed-forward/feedback control with P and v_r as controlled outputs can be seen as the dash-dotted line in Figs. 3 through 6. In this case the P stays very close to the desired set point, and the effects of the disturbance on pressure and retentate velocity are largely damped out. To maintain this pressure, however, the bypass velocity, v_b, now varies to a large degree to act as a buffer and absorb the effects of the disturbance. The manipulated input e_{v1} varies widely to accomplish this. This type of feed-forward/feedback control is the best to use in a situation where the plant is operating close to the high pressure constraints, which is usually the case at very high recoveries. This type of control is desirable because the bypass velocity can vary widely with little to no ill-effects on the system: v_b is readily recycled, there are usually no downstream lines that depend on v_b, and there are no safety issues associated with wide v_b variations.

V. CONCLUSIONS

The goal of this work was to develop model based nonlinear feed-forward/feedback control structures for high recovery RO desalination while accounting for such practical issues as sampled measurements and large time-varying feed disturbances. In order to accomplish this goal a detailed mathematical model of a high-recovery RO plant was first developed. The proposed model adequately describes the evolution of high recovery process states in time, and also accounts for the spatial variation of TDS and flow-rate inside the membrane unit. Nonlinear Lyapunov-based feedback and feed-forward controllers were implemented on the high recovery RO system in three simulation examples. The additional feed-forward component in the controller was able to compensate for large time varying disturbances in the feed concentration.

REFERENCES

[1] A. Rahardianto, J. Gaoa, C. J. Gabelich, M. D. Williams, and Y. Cohen, "High recovery membrane desalting of low-salinity brackish water: Integration of accelerated precipitation softening with membrane ro," *J. Membrane Sci.*, vol. 289, pp. 123–137, 2007.

[2] J. K. Kimes, "The regulation of concentrate disposal in florida," *Desalination*, vol. 102, pp. 87–92, 1995.

[3] M. Aboabboud and S. Elmasallati, "Potable water production from seawater by the reverse osmosis technique in libya," *Desalination*, vol. 203, pp. 119–133, 2007.

[4] J. Chen, F. Wang, M. Meybeck, D. He, X. Xia, and L. Zhang, "Spatial and temporal analysis of water chemistry records (19582000) in the huanghe (yellow river) basin," *Global Biogeochem. Cycles*, vol. 19, p. GB3016, 2005.

[5] I. M. Alatiqi, A. H. Ghabris, and S. Ebrahim, "System identification and control of reverse osmosis desalination," *Desalination*, vol. 75, pp. 119–140, 1989.

[6] M. W. Robertson, J. C. Watters, P. B. Desphande, J. Z. Assef, and I. Alatiqi, "Model based control for reverse osmosis desalination processes," *Desalination*, vol. 104, pp. 59–68, 1996.

[7] A. Abbas, "Model predictive control of a reverse osmosis desalination unit," *Desalination*, vol. 194, pp. 268–280, 2006.

[8] J. Z. Assef, J. C. Watters, P. B. Deshpande, and I. M. Alatiqi, "Advanced control of a reverse osmosis desalination unit," *J. Proc. Contr.*, vol. 7, pp. 283–289, 1997.

[9] A. C. Burden, P. B. Deshpande, and J. C. Watters, "Advanced control of a b-9 permasep permeator desalination pilot plant," *Desalination*, vol. 133, pp. 271–283, 2001.

[10] C. K. Liu, J.-W. Park, R. Migita, and G. Qin, "Experiments of a prototype wind-driven reverse osmosis desalination system with feedback control," *Desalination*, vol. 150, pp. 277–287, 2002.

[11] D. Herold and A. Neskakis, "A small PV-driven reverse osmosis desalination plant on the island of Gran Canaria," *Desalination*, vol. 137, pp. 285–292, 2001.

[12] A. Gambier and E. Badreddin, "Application of hybrid modeling and control techniqeues to desalination plants," *Desalination*, vol. 152, pp. 175–184, 2002.

[13] J. M. Dickson, J. Spencer, and M. L. Costa, "Dilute single and mixed solute systems in a spiral wound reserve osmosis module part i: Theoretical model development," *Desalination*, vol. 89, pp. 63–88, 1992.

[14] C. W. McFall, P. D. Christofides, Y. Cohen, and J. F. Davis, "Fault-tolerant control of a reverse osmosis desalination process," in *8th internation IFAC Symposium on Dynamics and Control of Process Systems Vol.3*, Cancun, Mexico, 2007, pp. 163–168.

[15] C. J. Geankoplis, *Transport Processes and Separation Process Principles, Fourth Edition*. Prentice Hall, 2003.

[16] Y. Lua, Y. Hua, X. Zhang, L. Wu, and Q. Liu, "Optimum design of reverse osmosis system under different feed concentration and product specification," *J. Membr. Sci.*, vol. 287, pp. 219–229, 2007.

[17] R. B. Bird, W. E. Stewart, and E. N. Lightfoot, *Transport Phenomena, Second Edition*. Wiley, 2002.

[18] S. C. Chapra and R. P. Canale, *Numerical Methods for Engineers, Fourth Edition*. McGraw Hill, 2002.

[19] Y. Lin and E. D. Sontag, "A universal formula for stabilization with bounded controls," *Sys. & Contr. Lett.*, vol. 16, pp. 393–397, 1991.

[20] N. H. El-Farra and P. D. Christofides, "Bounded robust control of constrained multivariable nonlinear processes," *Chem. Eng. Sci.*, vol. 58, pp. 3025–3047, 2003.

[21] P. Christofides and N. El-Farra, *Control of nonlinear and hybrid process systems: designs for uncertainty, constraints and time delays*. Springer, 2004.